"With PerFRACTION, we've shown that **large-scale clinical implementation of in vivo transit dosimetry is feasible**, even for complex techniques."

Evy Bossuyt, M.Sc.,
Iridium Netwerk

SunCHECK® In-Vivo QA In Action

Over a span of 4 years, Iridium Netwerk's workflow adjustments — following the start of an In-Vivo QA program with SunCHECK® — resulted in consistent reductions in failed fractions.*

With automated in-vivo monitoring, SunCHECK helps clinical teams efficiently identify and address issues, in support of continuous improvement.

**Assessing the impact of adaptations to the clinical workflow using transit in vivo dosimetry E. Bossuyt, et al., Iridium Netwerk, Medical Physics, Antwerpen, Belgium, Physics and Imaging in Radiation Oncology 25 (2023) 100420*

Learn how >

sunnuclear.com

SUN NUCLEAR
A MIRION MEDICAL COMPANY

Received: 16 December 2022 | Revised: 13 July 2023 | Accepted: 11 September 2023

DOI: 10.1002/mp.16757

RESEARCH ARTICLE

MEDICAL PHYSICS

Diamond detectors for dose and instantaneous dose-rate measurements for ultra-high dose-rate scanned helium ion beams

Thomas Tessonnier[1,2] | **Gianluca Verona-Rinati**[3] | **Luisa Rank**[1,4] | **Rafael Kranzer**[5,6] | **Andrea Mairani**[1,2,7] | **Marco Marinelli**[3]

[1]Heidelberg Ion Beam Therapy Center (HIT), Department of Radiation Oncology, Heidelberg University Hospital, Heidelberg, Germany

[2]Clinical Cooperation Unit Translational Radiation Oncology, German Cancer Consortium (DKTK) Core-Center Heidelberg, National Center for Tumor Diseases (NCT), Heidelberg University Hospital (UKHD) and German Cancer Research Center (DKFZ), Heidelberg, Germany

[3]Industrial Engineering Department, University of Rome Tor Vergata, Rome, Italy

[4]Faculty of Physics, Karlsruhe Institute of Technology (KIT), Karlsruhe, Germany

[5]PTW-Freiburg, Freiburg, Germany

[6]University Clinic for Medical Radiation Physics, Medical Campus Pius Hospital, Carl von Ossietzky University, Oldenburg, Germany

[7]Medical Physics department, National Centre of Oncological Hadrontherapy (CNAO), Pavia, Italy

Correspondence
Thomas Tessonnier, Heidelberg Ion Beam Therapy Center (HIT), Department of Radiation Oncology, Heidelberg University Hospital, Heidelberg, Germany.
Email: thomas.tessonnier@med.uni-heidelberg.de

Abstract

Background: The possible emergence of the FLASH effect—the sparing of normal tissue while maintaining tumor control—after irradiations at dose-rates exceeding several tens of Gy per second, has recently spurred a surge of studies attempting to characterize and rationalize the phenomenon. Investigating and reporting the dose and instantaneous dose-rate of ultra-high dose-rate (UHDR) particle radiotherapy beams is crucial for understanding and assessing the FLASH effect, towards pre-clinical application and quality assurance programs.

Purpose: The purpose of the present work is to investigate a novel diamond-based detector system for dose and instantaneous dose-rate measurements in UHDR particle beams.

Methods: Two types of diamond detectors, a microDiamond (PTW 60019) and a diamond detector prototype specifically designed for operation in UHDR beams (flashDiamond), and two different readout electronic chains, were investigated for absorbed dose and instantaneous dose-rate measurements. The detectors were irradiated with a helium beam of 145.7 MeV/u under conventional and UHDR delivery. Dose-rate delivery records by the monitoring ionization chamber and diamond detectors were studied for single spot irradiations. Dose linearity at 5 cm depth and in-depth dose response from 2 to 16 cm were investigated for both measurement chains and both detectors in a water tank. Measurements with cylindrical and plane-parallel ionization chambers as well as Monte-Carlo simulations were performed for comparisons.

Results: Diamond detectors allowed for recording the temporal structure of the beam, in good agreement with the one obtained by the monitoring ionization chamber. A better time resolution of the order of few μs was observed as compared to the approximately 50 μs of the monitoring ionization chamber. Both diamonds detectors show an excellent linearity response in both delivery modalities. Dose values derived by integrating the measured instantaneous dose-rates are in very good agreement with the ones obtained by the standard electrometer readings. Bragg peak curves confirmed the consistency of the charge measurements by the two systems.

Conclusions: The proposed novel dosimetric system allows for a detailed investigation of the temporal evolution of UHDR beams. As a result, reliable and accurate determinations of dose and instantaneous dose-rate are possible, both required for a comprehensive characterization of UHDR beams and relevant for FLASH effect assessment in clinical treatments.

KEYWORDS
diamond detector, FLASH, instantateneous dose-rate, particle therapy, ultra-high dose-rate

1 | INTRODUCTION

FLASH radiotherapy promises an enhancement of the radiotherapy therapeutic window with increased normal tissue sparing and without any loss of tumor control. Several studies have been investigating the FLASH effect over the last decade with in-vitro and in-vivo experiments.[1–10] Recently, the first proton FLASH clinical trial was completed,[11] and other studies and trials are planned, for skin tumor or bones metastasis.[4,11–13] While the overall FLASH mechanisms are not fully understood,[14] some key factors are playing a crucial role for obtaining the FLASH effect, such as the oxygen level of the cells and the surrounding medium as well as the dose and dose-rates delivered during the treatment.[10,15] As for the two latter quantities, directly linked to the beam delivery modality, a minimum dose of ∼10 Gy and an ultra-high dose-rate (UHDR) of at least 40 Gy/s have been reported to be needed to observe the FLASH sparing effect.[16–18] The spatiotemporal dose distribution, either predicted or measured, represents decisive information to assess the FLASH effect, regardless of the particle used in the irradiation procedure. Most of the studies on FLASH are based on electron beams.[1,2] Experiments with heavier particles were performed as well, mainly with protons[9,19–22] and more sparsely with helium[8] and carbon ions.[23]

Different methods of ultra-high dose-rate ion beam delivery are possible and are impacting the spatiotemporal dose-rate distribution depending on:

1. The accelerator type[24,25]: (i) cyclotron isochronous (quasi-continuous radiation with ∼100 MHz pulses); (ii) synchrocyclotron (pulsed irradiation with ∼100 MHz micro-pulses and ∼1 kHz macro-pulses); (iii) synchrotron (pulsed irradiation with spills of ∼1 MHz "micro-bunches" and <1 Hz pulses);
2. The lateral delivery[26–28]: (i) passive scattering or pencil beam scanning and (ii) in-depth delivery (Bragg peak with or without beam modifier).

Regarding these aspects, the one which might have the most relevant impact on the FLASH sparing capabilities might be linked to the lateral delivery with pencil beam scanning.[27] The distributions of the individual spots over the time lead to a complex instantaneous dose-rate distribution as well as to the need of a new dose-rate definition, somehow correlated to the normal tissue sparing. Several concepts of dose-rate can be found in the literature[27–29] and could be implemented in dedicated dose and dose-rate engines. Thus, the importance of an accurate model for dose and dose-rate distribution predictions is of utmost importance and needs to be benchmarked against measurements. Quality assurance for FLASH-based planning systems will need verification measurements of the dose-rate distribution in addition to the standard dose verification as usually done in clinical routine. Therefore, dedicated detectors with excellent dose accuracy and time-resolution are needed. In addition, as compared to electron or photon therapy, particle therapy is characterized by high values of the linear energy transfer (LET) (of the order of 20 keV/μm for helium ions and 100 keV/μm for carbon ions) thus requiring the availability of detectors having a LET independent response.

Several detectors are envisioned to work for FLASH radiation therapy,[30–32] from strip detectors to diamond detectors. PTW microDiamond detectors (mD)[33,34] have already been successfully tested under high LET conditions for standard dose-rate delivery (SDR).[35,36] Compared to other detectors they present the advantage to be tissue equivalent, with an excellent time and spatial resolution. Recently, a novel type of diamond detector prototype, the flashDiamond (fD) has been introduced to overcome nonlinearity issue observed for ion chambers and solid-state detectors in ultra-high dose-per-pulse and UHDR conditions.[37,38]

In this study, a novel dosimetric system is proposed, based on mD or fD detectors, for both dose and instantaneous dose-rate measurements, aimed at a comprehensive characterization of UHDR beams. Such devices were investigated under ultra-high dose-rate helium ion beam irradiation.

2 | MATERIALS AND METHODS

2.1 | Irradiation facility

The Heidelberg ion beam therapy center (HIT) is a synchrotron-based facility providing proton, helium ions, and carbon ions for patient treatment. Oxygen beams can be delivered as well for research purposes. With the increase of interest in FLASH application, the HIT facility has made available the possibility to increase the ion delivery performance by tuning beam extraction toward resonance point and increasing to higher power level the radiofrequency-knockout exciter.[8,23,39] In addition, the beam monitoring system ionization chamber (MIC) gas was exchanged from $ArCO_2$ mixture to a helium gas mixture to reduce saturation and non-linearity of the dose response occurring at UHDR.[23,40] At high doses, these parameters ensure to provide a relatively good agreement between SDR irradiation (<0.1–0.01 Gy/s)

and UHDR delivery (>40 Gy/s). UHDR delivery in the research room is achieved by setting a higher value to the beam current in a specific particle beam plan (ion type, energy, spots position, number of particles per spot, beam current). These specific settings resulted in an increased power level of the knockout exciter through the feedback of the intensity control system, and thus UHDR delivery. The particle fluence was recorded by the MIC located at the end of the beamline, having a 50 μs integration time. For helium ion UHDR delivery, the maximum number of particles deliverable in a single spill of hundreds of milliseconds is about 2.5×10^9 ions.

2.2 | Diamond detectors and electronic chain for dose and instantaneous dose-rate measurements

Two diamond detectors were utilized: a microDiamond (mD) detector (60019, PTW Freiburg)[33,34] and a so called "flashDiamond" (fD) detector prototype.[37,38] The mD detector is based on a diamond Schottky diode, whose sensitive volume is a cylinder 2.2 mm in diameter, 1 μm thick. The fD detector prototype has a structure similar to the one of the mD detectors but its design was specifically optimized for operation in UHDR and ultra-high dose-per pulse conditions. Such a device was proven to produce a linear response under 4 μs pulsed electron beams up to more than 20 Gy/pulse, corresponding to an instantaneous dose-rate of about 5 MGy/s. The device has a sensitive volume 1.1 mm in diameter, 1 μm thick, and is encapsulated in a housing nearly identical to the one of the mD detector.

Two different electronic chains were utilized for absorbed dose and instantaneous dose-rate measurements with the diamond detectors:

1. For dose measurements only, the diamond detectors were coupled to a PTW UNIDOS Webline electrometer;
2. For instantaneous dose-rate measurements, the diamond detectors were connected to a variable gain transimpedance amplifier (model DLPCA 200, FEMTO, Germany) and then to a 12 bit 200 MHz digital oscilloscope (PicoScope 5444A, Pico Technology, UK). A 10^6 V/A gain of the transimpedance amplifier was adopted for the measurements with the mD detector. In this condition the FEMTO amplifier exhibits a 200 kHz bandwidth. The measurements with the fD detector were acquired by adopting a 10^7 V/A gain of the amplifier, resulting in a bandwidth of 50 kHz. Instantaneous dose-rate measurements could then as well be integrated to provide dose at the investigated position.

2.3 | Ionization chambers for dose measurements

In addition to the diamond detectors, two ionization chambers were used as reference detectors, a Pin-Point chamber (PPC) (31015, PTW Freiburg) and an Advanced Markus Chamber (AMC) (34045, PTW Freiburg), connected to the UNIDOS electrometer and providing only dose measurements. The PPC was used in this work as the reference detector for dose linearity investigation in the plateau region of the Bragg Peak, since this detector is currently used at HIT for dosimetry assessment before in vitro and in vivo UHDR experiments.[8] However, the AMC, a parallel plane chamber with a 1 mm in-depth electrode air gap is more adapted for in-depth dose measurements.

2.4 | Measurements setup

The measurement setup involved a water tank with a 3D motorized chamber holder (MP3, PTW Freiburg) with its entrance windows set 10 cm before the isocenter. Each detector was provided with a dedicated holder.

2.5 | Irradiation details

Two different set of plans were used, a single spot plan and a 2×2 cm^2 field plan (121 raster-scanned spots). The initial energy of the helium ions in both plans was set to 145.7 MeV/u and a ripple filter was introduced at the end of the beamline (Bragg peak range of about 14.5 cm in water).[8] The ripple filter is used to broaden the helium peak of 1–2 mm in depth[41] and is used as in current FLASH experiment at HIT and clinical routine.[8,42]

2.5.1 | Single spot irradiations

The first set of plans consisted of single spot with different number of particles. These plans were used to investigate:

1. the consistency of the temporal current response evolution of the diamond detectors in UHDR delivery against the MIC records;
2. the linearity response of the diamonds and electronic chains under UHDR delivery for different initial number of particles.

All measurements were performed at a depth of 5 cm in water after careful positioning of the detectors with in-line and cross-line profiles. The position was chosen to provide a good reproducibility between each

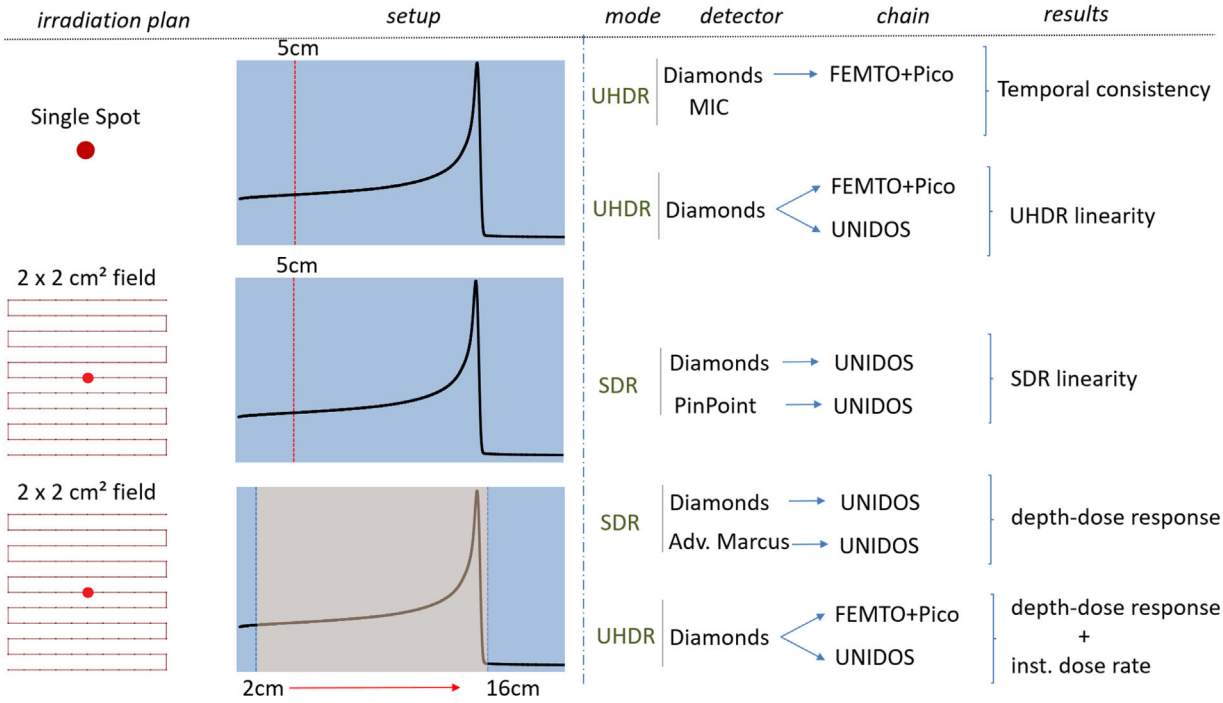

FIGURE 1 Overview of the experiments performed under different conditions together with their investigated endpoints. The UNIDOS chain represents the electronic dose chain measurements while the "FEMTO+Pico" chain is representative of the instantaneous dose-rate measurement chain. MIC stands for the monitoring ionization chamber.

measurement by staying in the plateau region of the Bragg peak curve with relatively small in-depth dose gradients and with a larger lateral dose distribution than at shallower depths.

For investigating the temporal current response measurements for UHDR delivery, the number of particles was set to 1×10^9, and the instantaneous dose-rate measurements chain was used with both fD and mD detectors. The measurements were then compared to the records of the MIC.

For the linearity investigations, the number of ions was defined in the plan between 4×10^8 and 2.5×10^9, the latter being close to the maximum number of ions deliverable within one UHDR spill. The linearity was investigated for both the dose and instantaneous dose-rate measurements chains.

Four repetitions were made for each investigated setting. The same UHDR current setting was used for all the spot plans. At 5 cm, the selected plans reached about 2.5–15 Gy in 40–250 ms.

2.5.2 | 2×2 cm^2 field irradiations

The second set of irradiations involved a 2×2 cm^2 field plan, consisting of 121 spots equally weighted with a 2 mm spot spacing (11×11 spots). This set was used to:

1. characterize the dose response linearity of the diamond detectors against PPC measurements at 5 cm under SDR irradiation;
2. evaluate the depth-dose response (from ~2 to ~16 cm in water) of the diamond detectors in SDR and UHDR conditions against AMC measurements in SDR.

For the linearity measurements in SDR, the detectors were set at 5 cm in water for dose varying between approximately 0.5 and 10 Gy, corresponding to a total number of particles of 5.6×10^8 to 1.1×10^{10}. Only the dose measurement chain (UNIDOS) was used. The detectors were positioned using in-line and cross-line profiles, and measurements were repeated four times for each dose level.

For the depth dependent investigations, the total number of particles of the 2×2 cm^2 field plan was set to 2.2×10^9. Irradiations were done in either SDR or UHDR. The current setting for UHDR was fixed for all irradiations, with a delivery time of 180 ms. Measurements were taken from ~2 to ~16 cm in water with the diamond detectors and the AMC. For the diamond detectors, measurements were performed with the dose and instantaneous dose-rate measurement chains in UHDR conditions, while only with the UNIDOS (dose measurement chain) only for SDR delivery. The measurements with the AMC were done only at SDR irradiation modality with the UNIDOS. Measurements performed with

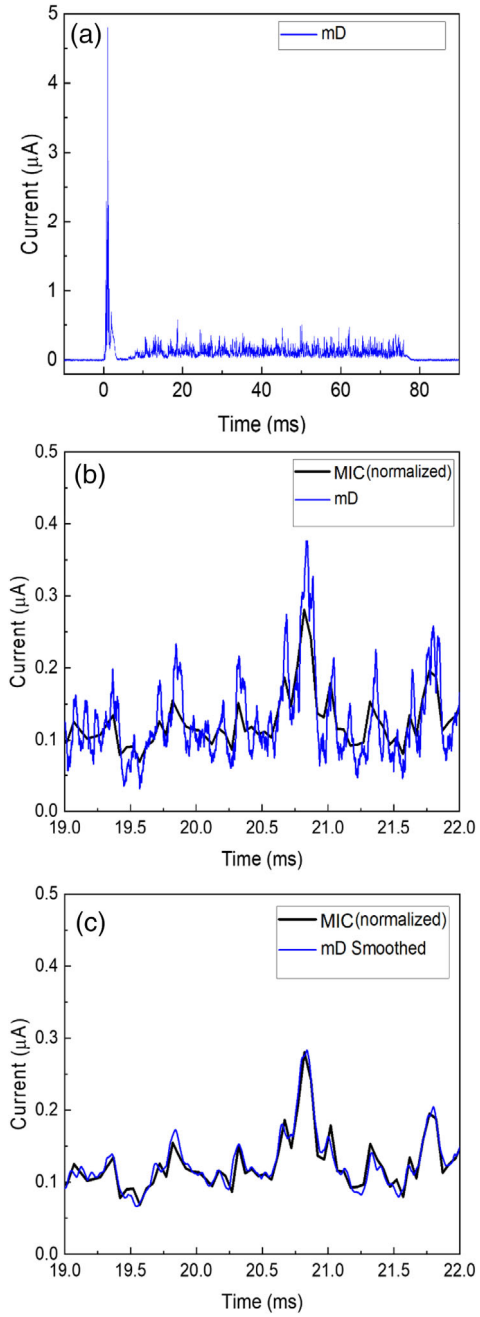

FIGURE 2 (a) microDiamond (mD) current during 10^9 ions spot irradiation in ultra-high dose-rate modality; (b) enlarged view compared with the signal from the monitoring ionization chamber (MIC); (c) comparison between the mD smoothed signal (1st order LP filter, 64 μs integration time) and the signal from the MIC.

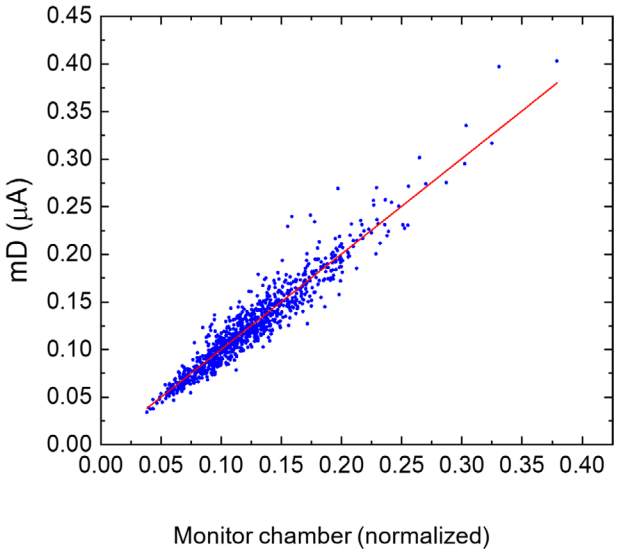

FIGURE 3 microDiamond (mD) smoothed current as a function of the monitor chamber signal.

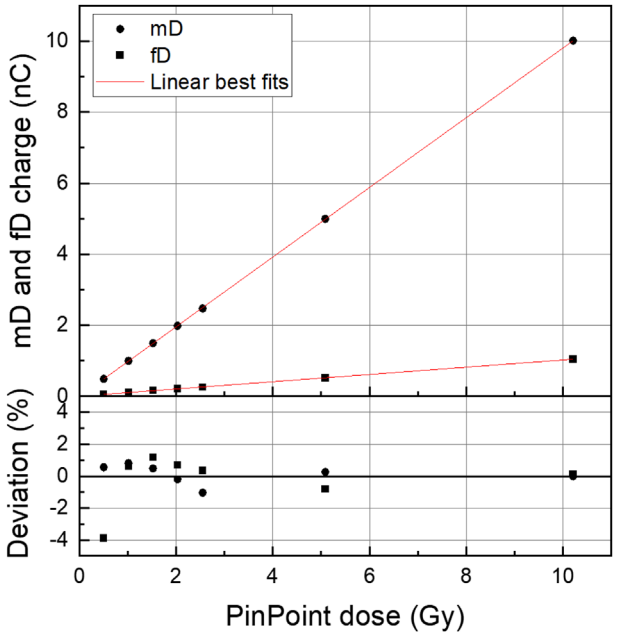

FIGURE 4 Linearity plot in standard dose-rate modality of the microDiamond (mD) and flashDiamond (fD) current as a function of the measured PinPoint dose at 5 cm in water.

the diamond detectors and instantaneous dose-rare measurement chains allow to record for each investigated depth the temporal evolution of the dose-rate along the irradiation of the 121 spots. Each measurement was repeated three times. In addition, Monte Carlo FLUKA[43,44] simulations of the depth dose **a** in the water tank were performed using a detailed geometry of the HIT beamline.[45] All simulations reached a statistical uncertainty under 0.5%.

3 | RESULTS AND DISCUSSION

An overview of the different performed experiments is presented in Figure 1.

At first, a comparison of the monitoring ionization chamber recordings against the ones from the mD detector at 5 cm in water was performed for a single spot delivery of 2×10^9 ions in UHDR conditions. The position standard deviation, to the central position, from the records of the beam monitoring system

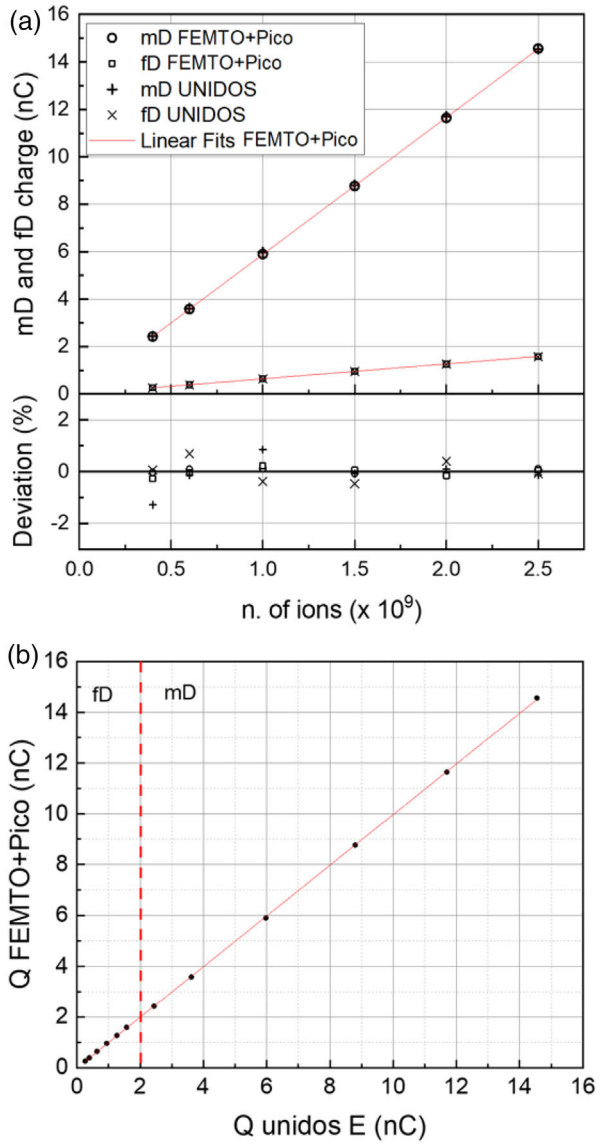

FIGURE 5 (a) Linearity plot in ultra-high dose-rate modality of the microDiamond (mD) and flashDiamond (fD) current at 5 cm in water as a function of the requested number of helium ions, for both measurement chains (UNIDOS electrometer or FEMTO+pico); (b) charge obtained by integrating the instantaneous detector current (FEMTO+Pico), from the flashDiamond (fD) and microdiamond (mD) as a function of the charge measured by the UNIDOS electrometer.

was <0.03 mm with no records showing deviation above 0.1 mm. Figure 2a presents the current from the mD detector as a function of time. Figure 2b displays an enlarged view of the signal reported in Figure 2a together with the one from the MIC. The two datasets were independently acquired, with no common trigger. Therefore, to better compare and analyze the temporal traces resulting from the two detectors, the signals were manually synchronized. Afterwards the amplitude of the MIC response was normalized to the diamond one. The fast response of the diamond detectors allows to appreciate more detailed structures of the dose-rate/current temporal evolution of the spill delivery than the MIC. The initial peak structure, present in all UHDR irradiation of this work in the signal recorded by both the MIC and diamond detectors, is linked to the beam extraction to achieved UHDR before being regulated by the intensity control system. The fine structure visible only with the diamond detectors are due to the fact that the extraction process is a stochastic process, leading to such fluctuations.

In order to allow a comparison between the two signals, the signal from the diamond detector was smoothed by applying an integrating filter. An optimal value of 64 μs integration time for the diamond detectors was found in order to achieve the best matching between the two signals. The result is shown in Figure 2c. The correlation between the two signals from Figure 2 is reported in Figure 3, in which 1000 values were extracted from the smoothed diamond signal and reported as a function of the respective acquisition values obtained by the MIC. Despite the presence of a certain amount of data scattering, mostly due to a not perfect matching between the temporal behavior of the two signals, a good linear relationship between the two devices is observed with a Pearson correlation coefficient $r = 0.995$. Similar results, not reported here, were observed by using the fD detector. All diamond measurements compared to MIC records presented Pearson correlation coefficients $r > 0.99$.

The sensitivities of the two devices were derived by the linearity test measured in SDR conditions by delivering all the above described 121 raster scanned spot plans. The results are reported in Figure 4. An excellent linearity can be appreciated for both detectors. The linear best fit is also reported (red line), resulting in sensitivities of (0.981 ± 0.002) and (0.102 ± 0.001) nC/Gy for the mD and fD detector respectively. The deviation from linearity is reported in the lower plot of Figure 4 for both devices, which was found to be within about 1%, with the only exception of the lowest dose where a deviation of about 4% was observed. At such low dose, the helium gas mixture used in the MIC for UHDR irradiation was leading to a loss of sensitivity and reproducibly of the delivery when a low number of particles were required per spots.

The linearity of detector responses were investigated as a function on the number of ions measured by the MIC, under UHDR delivery using the single spot plans. The results are summarized in Figure 5a for both the detectors and readout electronic acquisition systems. The charge values from the "FEMTO+Pico" chain were obtained by the integral of the recorded signal, divided by the nominal gain of the FEMTO amplifier. Again, a good linearity is observed in all cases with deviations from the linear best fit being less than about 1.3%.

A comparison between the responses of two readout chain is shown in Figure 5b, in which the integrated

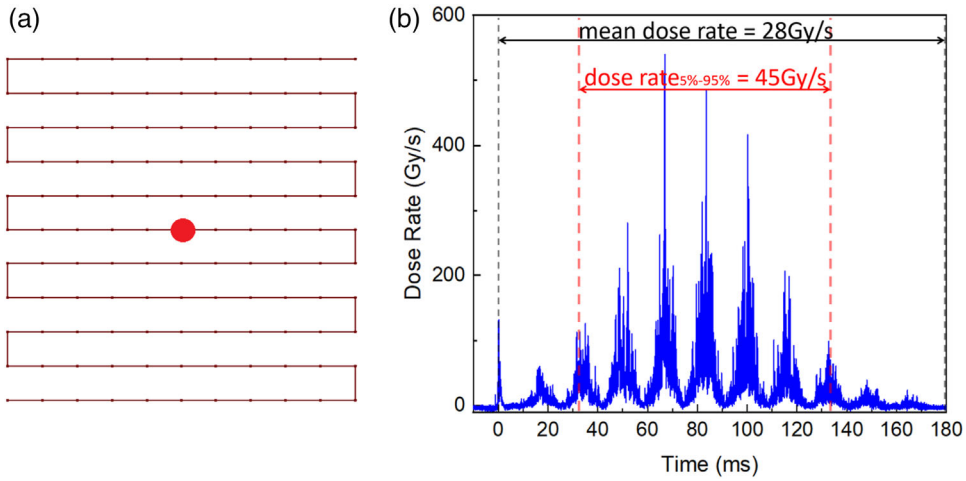

FIGURE 6 (a) A representation of the 2 × 2 cm^2 field plan, with the measurement detectors located in the middle of the field. (b) microDiamond instantaneous dose-rate evolution, during a 2 × 2 cm^2 scanned beam (121 spots) measured at 14 cm in water in ultra-high dose-rate condition in the center of the irradiation field. Two dose-rate metrics are displayed, the mean dose rate and the dose rate$_{5\%-95\%}$.

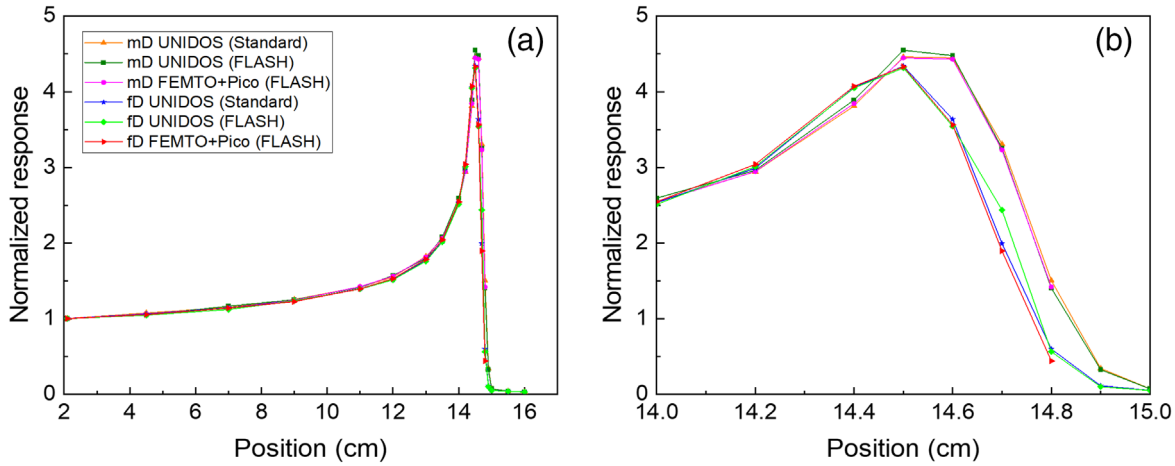

FIGURE 7 Bragg peak as measured by the two detectors (microDiamonds [mD] and flashDiamonds [fD]) both by using the UNIDOS electrometer or by integrating the FEMTO+Pico signal, in either ultra-high dose-rate (FLASH) or standard delivery conditions.

charge values from the FEMTO+Pico chain for both detectors are reported as a function of the charge measured by using the UNIDOS electrometer. A very good linear behavior is observed with a slope of 0.997, implying that no additional correction factors are needed to accurately record the dose-rate temporal evolution. An example is reported in Figure 6b, where the temporal evolution of the dose-rate measured by the mD at 14 cm depth in water for the 121 spots plan with 2.2 × 10^9 total particle numbers delivered in UHDR conditions is shown. Eleven individual peaks can be identified corresponding to the contribution of pencil beams from the 11 lines of the plan (Figure 6a). The instantaneous dose-rate evolution is shown over the whole delivery time (about 180 ms) with a maximum value of about 550 Gy/s. The standard approach for mean dose-rate calculation (total dose of about 5 Gy divided by the overall delivery time) lead to a mean dose-rate about 28 Gy/s instead. By adopting a different dose-rate definition proposed in the recent literature for FLASH experiments,[29] in which an adjusted time window (~100 ms), by omitting the delivered first 5% and last 5% of the total dose at the measurement point, corresponding to the 90% of the delivered dose is considered for the dose-rate calculation. In such dose-rate framework a dose-rate 5%–95% value of 45 Gy/s is obtained. Such large differences deriving from different dose-rate definitions in combination with huge variations of the measured instantaneous dose-rate, show the importance of an accurate dose-rate evaluation for scanned ion beam FLASH investigations and FLASH-TPS modeling.

The depth dose responses of the two detectors were measured both in SDR and UHDR modality, by using both the electronic chains in UHDR condition

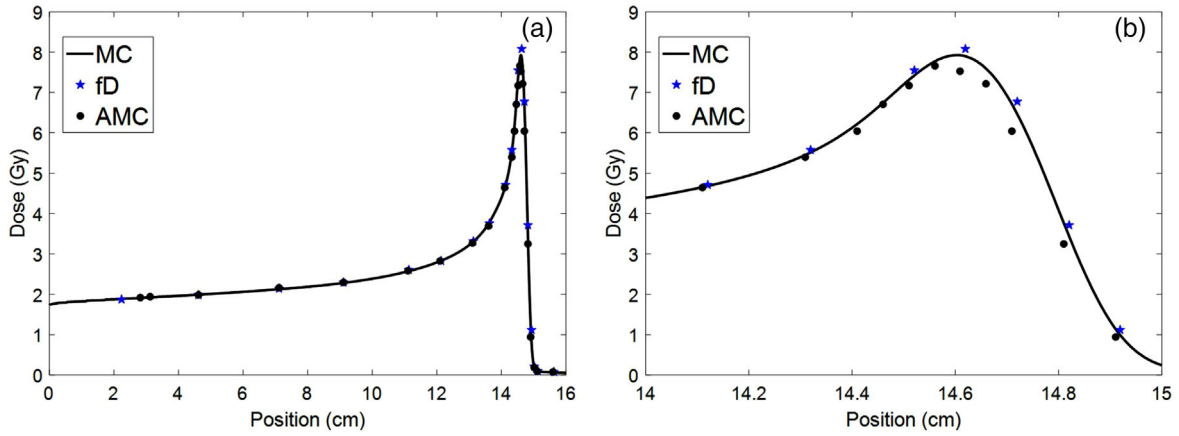

FIGURE 8 Bragg peak as measured by the flashDiamond (fD) and Advanced Markus Chamber (AMC), and simulated with the Monte-Carlo FLUKA (MC).

and the UNIDOS electrometer only in SDR conditions. The results, normalized at 2 cm depth, are reported in Figure 7. No significant differences were observed between the two acquisition chains, thus demonstrating the equivalence of the two systems. However, some small discrepancies can be appreciated between the two detectors. In particular, the mD shows an about 4% higher response in the Bragg peak region. In addition, all the fD curves appear to be translated of about 0.5 mm towards the entrance direction with respect to the mD ones, probably due to a positioning error. In Figure 8 the absolute dose measurements as a function of the depth are reported for the fD and compared to the ones from the AMC and the MC simulation. It can be observed that the fD (and mD) exhibit a higher response in the region close to the Bragg peak as compared to the AMC, while the MC simulation provides intermediate results. More specific experiments are in progress to evaluate a potential LET dependences of the diamond detector response. Nevertheless, the results, shown in Figures 7 and 8, strongly support the feasibility of absolute dose and dose-rate measurements by the proposed acquisition system.

4 | CONCLUSIONS

Investigating and reporting the acquired dose-rate is crucial in understanding and sharing the results of potential FLASH effect. The proposed dosimetric system allows for accurate dose and dose-rate measurements in SDR and UHDR delivery modes. Both the microDiamond and the recently proposed flashDiamond detectors are suitable for dose-rate measurements in UHDR ion therapy beams.

ACKNOWLEDGMENTS

This work was supported in part by NIH-1P01CA257904-01A1. This project 18HLT04 UHDpulse has received funding from the EMPIR programme co-financed by the Participating States and from the European Union's Horizon 2020 research and innovation programme.

The authors would like to thank Dr. Schömers from the HIT accelerator team for his support and fruitful discussions.

CONFLICT OF INTEREST

Rafael Kranzer is a PTW employee while Marco Marinelli and Gianluca Verona Rinati, signed a contract with PTW-Freiburg involving financial interests deriving from the PTW diamond detectors commercialization.

REFERENCES

1. Favaudon V, Caplier L, Monceau V, et al. Ultrahigh dose-rate FLASH irradiation increases the differential response between normal and tumor tissue in mice. *Sci Transl Med*. 2014;6(245):245ra93. doi:10.1126/SCITRANSLMED.3008973
2. Montay-Gruel P, Petersson K, Jaccard M, et al. Irradiation in a flash: unique sparing of memory in mice after whole brain irradiation with dose rates above 100 Gy/s. *Radiother Oncol*. 2017;124(3):365-369. doi:10.1016/j.radonc.2017.05.003
3. Vozenin MC, De Fornel P, Petersson K, et al. The advantage of FLASH radiotherapy confirmed in mini-pig and cat-cancer patients. *Clin Cancer Res*. 2019;25(1):35-42. doi:10.1158/1078-0432.CCR-17-3375
4. Bourhis J, Sozzi WJ, Jorge PG, et al. Treatment of a first patient with FLASH-radiotherapy. *Radiother Oncol*. 2019;139:18-22. doi:10.1016/j.radonc.2019.06.019
5. Montay-Gruel P, Bouchet A, Jaccard M, et al. X-rays can trigger the FLASH effect: ultra-high dose-rate synchrotron light source prevents normal brain injury after whole brain irradiation in mice. *Radiother Oncol*. 2018;129(3):582-588. doi:10.1016/j.radonc.2018.08.016
6. Levy K, Natarajan S, Wang J, et al. Abdominal FLASH irradiation reduces radiation-induced gastrointestinal toxicity for the

treatment of ovarian cancer in mice. *Sci Rep*. 2020;10(1):21600. doi:10.1038/s41598-020-78017-7
7. Diffenderfer ES, Verginadis II, Kim MM, et al. Design, implementation, and in vivo validation of a novel proton FLASH radiation therapy system. *Int J Radiat Oncol Biol Phys*. 2020;106(2):440-448. doi:10.1016/j.ijrobp.2019.10.049
8. Tessonnier T, Mein S, Walsh DWM, et al. FLASH dose rate helium ion beams: first in vitro investigations. *Int J Radiat Oncol Biol Phys*. 2021;111(4):1011-1022. doi:10.1016/j.ijrobp.2021.07.1703
9. Dokic I, Meister S, Bojcevski J, et al. Neuroprotective effects of ultra-high dose rate FLASH Bragg peak proton irradiation. *Int J Radiat Oncol*. 2022;113(3):614-623. doi:10.1016/j.ijrobp.2022.02.020
10. Vozenin MC, Bourhis J, Durante M. Towards clinical translation of FLASH radiotherapy. *Nat Rev Clin Oncol*. 2022;19(12):791-803. doi:10.1038/s41571-022-00697-z
11. Mascia AE, Daugherty EC, Zhang Y, et al. Proton FLASH radiotherapy for the treatment of symptomatic bone metastases: the FAST-01 nonrandomized trial. *JAMA Oncol*. 2023;9(1):62-69. doi:10.1001/jamaoncol.2022.5843
12. Gaide O, Herrera F, Jeanneret Sozzi W, et al. Comparison of ultra-high versus conventional dose rate radiotherapy in a patient with cutaneous lymphoma. *Radiother Oncol*. 2022;174:87-91. doi:10.1016/J.RADONC.2021.12.045
13. Taylor PA, Moran JM, Jaffray DA, Buchsbaum JC. A roadmap to clinical trials for FLASH. *Med Phys*. 2022;49(6):4099-4108. doi:10.1002/MP.15623
14. Wilson JD, Hammond EM, Higgins GS, Petersson K. Ultra-high dose rate (FLASH) radiotherapy: silver bullet or fool's gold? *Front Oncol*. 2020;9:1563. doi:10.3389/fonc.2019.01563
15. Esplen N, Mendonca MS, Bazalova-Carter M. Physics and biology of ultrahigh dose-rate (FLASH) radiotherapy: a topical review. *Phys Med Biol*. 2020;65(23):23TR03. doi:10.1088/1361-6560/abaa28
16. van Marlen P, Dahele M, Folkerts M, Abel E, Slotman BJ, Verbakel WFAR. Bringing FLASH to the clinic: treatment planning considerations for ultrahigh dose-rate proton beams. *Int J Radiat Oncol Biol Phys*. 2020;106(3):621-629. doi:10.1016/j.ijrobp.2019.11.011
17. Bourhis J, Montay-Gruel P, Gonçalves Jorge P, et al. Clinical translation of FLASH radiotherapy: why and how? *Radiother Oncol*. 2019;139:11-17. doi:10.1016/j.radonc.2019.04.008
18. Vozenin MC, Hendry JH, Limoli CL. Biological benefits of ultra-high dose rate FLASH radiotherapy: sleeping beauty awoken. *Clin Oncol*. 2019;31(7):407-415. doi:10.1016/j.clon.2019.04.001
19. Beyreuther E, Brand M, Hans S, et al. Feasibility of proton FLASH effect tested by zebrafish embryo irradiation. *Radiother Oncol*. 2019;139:46-50. doi:10.1016/j.radonc.2019.06.024
20. Buonanno M, Grilj V, Brenner DJ. Biological effects in normal cells exposed to FLASH dose rate protons. *Radiother Oncol*. 2019;139:51-55. doi:10.1016/j.radonc.2019.02.009
21. Singers SB, Krzysztof Sitarz M, Ankjaergaard C, et al. In vivo validation and tissue sparing factor for acute damage of pencil beam scanning proton FLASH. *Radiother Oncol*. 2022;167:109-115. doi:10.1016/j.radonc.2021.12.022
22. Patriarca A, Fouillade C, Auger M, et al. Experimental set-up for FLASH proton irradiation of small animals using a clinical system. *Int J Radiat Oncol Biol Phys*. 2018;102(3):619-626. doi:10.1016/j.ijrobp.2018.06.403
23. Tinganelli W, Sokol O, Quartieri M, et al. Ultra-high dose rate (FLASH) carbon ion irradiation: dosimetry and first cell experiments. *Int J Radiat Oncol Biol Phys*. 2022;112(4):1012-1022. doi:10.1016/J.IJROBP.2021.11.020
24. Farr J, Grilj V, Malka V, Sudharsan S, Schippers M. Ultra-high dose rate radiation production and delivery systems intended for FLASH. *Med Phys*. 2022;49(7):4875-4911. doi:10.1002/MP.15659
25. Darafsheh A, Hao Y, Zwart T, et al. Feasibility of proton FLASH irradiation using a synchrocyclotron for preclinical studies. *Med Phys*. 2020;47(9):4348-4355. doi:10.1002/MP.14253
26. Kang M, Wei S, Isabelle Choi J, Simone CB, Lin H. Quantitative assessment of 3D dose rate for proton pencil beam scanning FLASH radiotherapy and its application for lung hypofractionation treatment planning. *Cancers*. 2021;13(14):3549. doi:10.3390/CANCERS13143549
27. Zou W, Diffenderfer ES, Cengel KA, et al. Current delivery limitations of proton PBS for FLASH. *Radiother Oncol*. 2021;155:212-218. doi:10.1016/J.RADONC.2020.11.002
28. Andreas Weber U, Scifoni E, Durante M. FLASH radiotherapy with carbon ion beams. *Med Phys*. 2022;49(3):1974-1992. doi:10.1002/MP.15135
29. Folkerts MM, Abel E, Busold S, Perez JR, Krishnamurthi V, Ling CC. A framework for defining FLASH dose rate for pencil beam scanning. *Med Phys*. 2020;47(12):6396-6404. doi:10.1002/MP.14456
30. Schüller A, Heinrich S, Fouillade C, et al. The European Joint Research Project UHDpulse—metrology for advanced radiotherapy using particle beams with ultra-high pulse dose rates. *Phys Medica*. 2020;80:134-150. doi:10.1016/J.EJMP.2020.09.020
31. Romano F, Bailat C, Jorge PG, Lerch MLF, Darafsheh A. Ultra-high dose rate dosimetry: challenges and opportunities for FLASH radiation therapy. *Med Phys*. 2022;49(7):4912-4932. doi:10.1002/MP.15649
32. Ashraf MR, Rahman M, Zhang R, et al. Dosimetry for FLASH radiotherapy: a review of tools and the role of radioluminescence and cherenkov emission. *Front Phys*. 2020;8:328. doi:10.3389/FPHY.2020.00328
33. Mandapaka AK, Ghebremedhin A, Patyal B, et al. Evaluation of the dosimetric properties of a synthetic single crystal diamond detector in high energy clinical proton beams. *Med Phys*. 2013;40(12):121702. doi:10.1118/1.4828777
34. Marinelli M, Prestopino G, Tonnetti A, et al. A novel synthetic single crystal diamond device for in vivo dosimetry. *Med Phys*. 2015;42(8):4636-4644. doi:10.1118/1.4926556
35. Marinelli M, Prestopino G, Verona C, et al. Dosimetric characterization of a microDiamond detector in clinical scanned carbon ion beams. *Med Phys*. 2015;42(4):2085-2093. doi:10.1118/1.4915544
36. Togno M, Nesteruk KP, Schäfer R, et al. Ultra-high dose rate dosimetry for pre-clinical experiments with mm-small proton fields. *Phys Medica*. 2022;104:101-111. doi:10.1016/j.ejmp.2022.10.019
37. Marinelli M, Felici G, Galante F, et al. Design, realization, and characterization of a novel diamond detector prototype for FLASH radiotherapy dosimetry. *Med Phys*. 2022;49(3):1902-1910. doi:10.1002/MP.15473
38. Verona Rinati G, Felici G, Galante F, et al. Application of a novel diamond detector for commissioning of FLASH radiotherapy electron beams. *Med Phys*. 2022;49(8):5513-5522. doi:10.1002/MP.15782
39. Schömers C, Brons S, Cee R, Peters A, Scheloske S, Haberer T. Beam Properties Beyond the Therapeutic Range at HIT; 2022.https://www.ipac23.org/preproc/doi/jacow-ipac2023-thpm064/index.html
40. Baack L, Schuy C, Brons S, et al. Reduction of recombination effects in large plane parallel beam monitors for FLASH radiotherapy with scanned ion beams. *Phys Med*. 2022;104:136-144. doi:10.1016/J.EJMP.2022.10.029
41. Tessonnier T, Mairani A, Brons S, Haberer T, Debus J, Parodi K. Experimental dosimetric comparison of 1H, 4He, 12C and 16O scanned ion beams. *Phys Med Biol*. 2017;62(10):3958-3982. doi:10.1088/1361-6560/aa6516
42. Tessonnier T, Ecker S, Besuglow J, et al. Commissioning of helium ion therapy and the first patient treatment with active beam delivery. *Int J Radiat Oncol*. 2023;116(4):935-948. doi:10.1016/J.IJROBP.2023.01.015
43. Böhlen TT, Cerutti F, Chin MPW, et al. The FLUKA code: developments and challenges for high energy and medical applications.

Nucl Data Sheets. 2014;120:211-214. doi:10.1016/j.nds.2014.07.049

44. Ferrari A, Sala PR, Fasso A, Ranft J. *FLUKA: A Multi-Particle Transport Code (Program Version 2005)*; 2005. doi:10.5170/cern-2005-010
45. Tessonnier T, Mairani A, Brons S, et al. Helium ions at the heidelberg ion beam therapy center: comparisons between FLUKA Monte Carlo code predictions and dosimetric measurements. *Phys Med Biol*. 2017;62(16):6784-6803. doi:10.1088/1361-6560/aa7b12

How to cite this article: Tessonnier T, Verona-Rinati G, Rank L, Kranzer R, Mairani A, Marinelli M. Diamond detectors for dose and instantaneous dose-rate measurements for ultra-high dose-rate scanned helium ion beams. *Med Phys*. 2023;1-10.
https://doi.org/10.1002/mp.16757